AEROFOIL MAXIMUM LIFT COEFFICIENT FOR MACH NUMBERS UP TO 0.4

1. NOTATION AND UNITS

		SI	*British*
$(a_1)_0$	slope of lift coefficient curve with incidence for aerofoil in incompressible flow	rad^{-1}	rad^{-1}
B_i	coefficients used in estimation of α_0 with $i = 1$ to 14 in Equation (5.1)	rad	rad
C_{Lm}	maximum lift coefficient of aerofoil		
C_{L0}	lift coefficient at zero incidence, Equation (5.3)		
ΔC_L	increment in lift coefficient (see Section 2.2)		
c	aerofoil chord	m	ft
F_1, F_2	parameters in Equation (7.1)		
F_M	factor for effect of Mach number on C_{Lm} (Equation (7.1))		
F_S	factor on C_{Lm} for modern aerofoils in Figure 5		
M	free-stream Mach number		
R_c	Reynolds number based on free-stream conditions and aerofoil chord		
t	maximum thickness of aerofoil	m	ft
t_b	trailing-edge base thickness (see Sketch 1.1)	m	ft
x	chordwise distance measured from aerofoil leading edge, positive rearwards	m	ft
x_{um}	value of x at which z_{um} occurs (see Sketch 1.1)	m	ft
z	aerofoil ordinate measured normal to chord, positive upwards (see Sketch 1.1)	m	ft
z_{ci}	aerofoil camber ordinate with $i = 1$ to 14 in Equation (5.1)	m	ft
z_l	lower-surface ordinate (see Sketch 1.1)	m	ft

Issued November 1984
Reprinted with Amendments A to C, January 1999
This page Amendment C

$z_l(x/c)$	lower-surface ordinate at x/c	m	ft
z_u	upper-surface ordinate (see Sketch 1.1)	m	ft
z_{um}	maximum upper-surface ordinate (see Sketch 1.1)	m	ft
$z_u(x/c)$	upper-surface ordinate at x/c	m	ft
$z_{u1.25}$	upper-surface ordinate at $x/c = 0.0125$	m	ft
α	incidence	rad	rad
α_0	zero-lift incidence, Equation (5.1)	rad	rad
τ_u	aerofoil upper-surface angle defined by Equation (3.1), see also Sketch 1.1	rad	rad

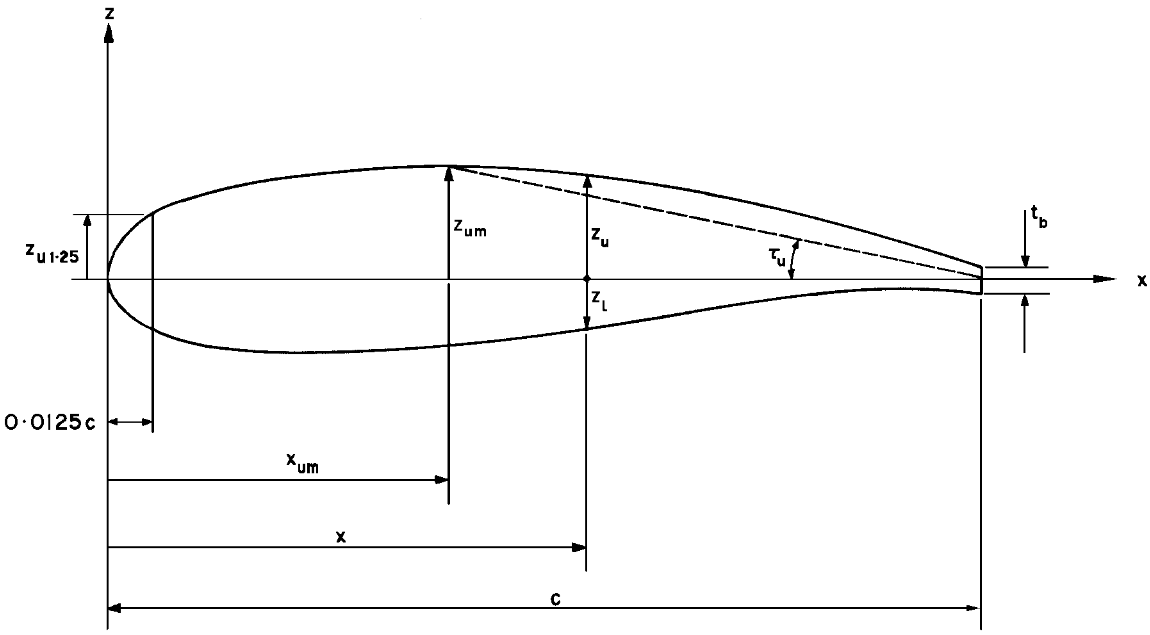

Sketch 1.1 Aerofoil geometry

2. INTRODUCTION

At low speeds the two-dimensional flow over an aerofoil normally remains attached at small incidences and the increase of lift with incidence is effectively linear, so that the lift coefficient at any incidence is given by the product of the lift-curve slope, $(a_1)_0$, and the incidence from zero lift, $(\alpha - \alpha_0)$. The variation of lift with incidence remains essentially linear until the onset of flow separation at a particular incidence, which is dependent on the free-stream conditions and aerofoil geometry. Further increase in incidence results in greater extents of flow separation and reduction in the slope of the lift-incidence curve until the total lift coefficient of the aerofoil reaches a maximum value (C_{Lm}) and the aerofoil stalls. At still higher incidences the lift is reduced, perhaps catastrophically.

2.1 Types of Stall

There are various types of stall related to where the flow separations occur on the aerofoil. The types of stall can be classified as follows.

(i) Trailing-edge stall, resulting from a trailing-edge flow separation which moves forward with increasing incidence.

(ii) Leading-edge stall, resulting from a sudden separation of the laminar boundary layer near the leading edge, due to the bursting of a small bubble, which generally occurs without subsequent flow reattachment.

(iii) Thin-aerofoil stall, which is due to a leading-edge separation reattaching to form a separation bubble. The reattachment point moves progressively aft with increasing incidence.

(iv) A combined trailing-edge and leading-edge stall.

Further details of these types of stall and the effect on the aerofoil force characteristics can be found in Derivations 4 and 7, and Reference 22.

For low speeds, and for aerodynamically smooth aerofoils, the type of stall has been found (Derivation 4) to depend on the Reynolds number and the value of the upper-surface ordinate of the aerofoil at the 0.0125 chord location, $z_{u1.25}$ (see Sketch 1.1).

For the correlation of aerofoil maximum lift coefficient it has been found necessary to consider the aerofoils in only two groups, those with $z_{u1.25}/c < 0.017$ and those with $z_{u1.25}/c \geq 0.017$. These groups can be considerd to contain aerofoils with predominantly leading-edge and trailing-edge stalls, respectively. Accordingly, the experimental values of C_{Lm} for the two groups have been correlated using leading-edge and trailing-edge geometrical parameters, respectively.

2.2 Scope of the Item

The main parameters that influence C_{Lm} are aerofoil geometry, surface condition (*i.e.* smooth or rough), Reynolds number and Mach number. Maximum lift coefficients are presented in terms of incremental lift coefficients, ΔC_L, added to the lift coefficient at zero incidence, C_{L0}, which is useful in its own right as a measure of the effect of camber on lift. This approach was adopted to account for the main influence of aerofoil camber on maximum lift so that data for cambered and symmetrical aerofoils could be considered together. Procedures for obtaining ΔC_L are given in Sections 3 and 4 for aerofoils with smooth and rough leading edges, while the procedure for obtaining C_{L0} is given in Section 5 and requires a detailed knowledge of the aerofoil geometry.

For the purposes of this Item a smooth aerofoil is defined as one with either no leading-edge roughness (*i.e.* natural boundary-layer transition) or with a small band of minimum roughness just sufficient to fix transition. This is the common practice for present day wind-tunnel tests; NASA, for example, use roughness boundary layer trips as illustrated in Sketch 2.1. A rough leading edge can be considered as similar to that obtained with ice formation or similar to that corresponding to the extent and size of roughness grains commonly used to fix boundary-layer transition in wind-tunnel tests of aerofoils at NACA some years ago, see Sketch 2.2a. Thus the data of Section 4, compared to those of Section 3, can be used as an indication of the loss in C_{Lm} due to ice formation.

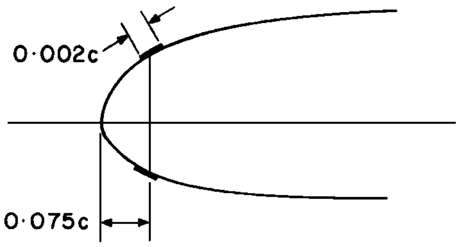

Sketch 2.1 Small-grain roughness for fixing boundary-layer transition in NASA tests (typically 0.0042 inch carborundum grains for a 24 inch chord model)

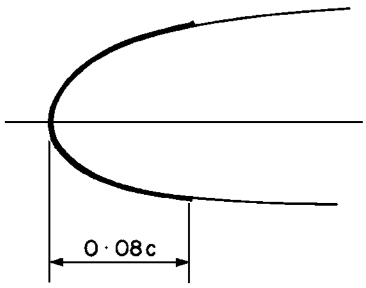

Sketch 2.2a

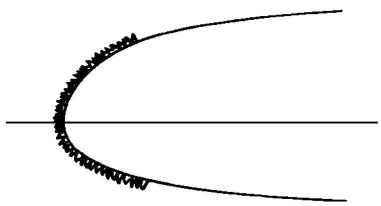

Sketch 2.2b

(a) Large-grain roughness for fixing boundary-layer transition in NACA tests (typically 0.011 inch carborundum grains for a 24 inch chord model, covering 5 to 10 per cent of treated surface area)

(b) Ice formation

A factor is given in Section 6 that has to be applied for modern, rear-loaded, aerofoils which terminate with a small trailing-edge base thickness and incorporate large rear camber as illustrated in Sketch 1.1. Finally, the effect of Mach number on C_{Lm}, for $M \le 0.4$, is obtained from Section 7.

To apply the method presented in this Item various aerofoil geometrical parameters are required that are defined with respect to the aerofoil chord line. For the purposes of this Item the chord line is defined as the straight line connecting the leading and trailing edges. For an aerofoil with a finite base thickness the trailing-edge point is taken as the mid-thickness point. The leading edge is defined as that unique point at which a circle centred at the trailing-edge point is tangential to the aerofoil.

This page Amendment C

The aerofoil maximum lift coefficient is obtained as follows:

$$C_{Lm} = (C_{L0} + \Delta C_L)F_S F_M \tag{2.1}$$

in which the increment ΔC_L is obtained from Section 3 or 4 and C_{L0} is obtained from Section 5. For modern aerofoils the factor F_S is obtained from Section 6 while for conventional sections $F_S = 1.0$. The factor F_M, obtained from Section 7, allows for the effect of Mach number up to 0.4. For $M \le 0.1$, $F_M = 1.0$.

A Fortran computer program for the method of this Item is available in ESDUpac A9315, see Item No. 93015 (Reference 23).

3. LIFT COEFFICIENT INCREMENT FOR AEROFOILS WITH SMOOTH LEADING EDGES

For aerofoils with smooth leading edges the lift coefficient increment, ΔC_L, in Equation (2.1) is obtained from Figure 1 or 2.

For aerofoils with $z_{u1.25}/c < 0.017$ Figure 1 gives ΔC_L as a function of $z_{u1.25}/c$ and Reynolds number, R_c. For $z_{u1.25}/c \ge 0.017$ Figure 2 gives ΔC_L as a function of $\tan\tau_u$ and Reynolds number, R_c. The quantity τ_u is the angle between the chord line and a line drawn from the maximum upper-surface ordinate to the trailing-edge point (see Sketch 1.1) given by

$$\tan\tau_u = (z_{um}/c)/(1 - x_{um}/c). \tag{3.1}$$

Figures 1 and 2 were obtained from measured data given in Derivations 2, 3, 5 to 8, 10 to 15, 17 to 20 which covered the ranges of parameters given in Table 3.1

TABLE 3.1
Ranges of Parameters for Tests on Aerofoils with Smooth Leading Edges

Parameter	*Range*
t/c	0.06 to 0.24
$z_{u1.25}/c$	0.0069 to 0.0563
$\tan\tau_u$	0.0429 to 0.2249
$R_c \times 10^{-6}$	0.7 to 9.0
M	0.09 to 0.47

4. LIFT COEFFICIENT INCREMENT FOR AEROFOILS WITH ROUGH LEADING EDGES

The data for aerofoils with rough leading edges are presented in a manner identical to those of Section 3 for aerofoils with smooth leading edges.

For aerofoils with $z_{u1.25}/c < 0.017$ Figure 3 gives ΔC_L as a function of $z_{u1.25}/c$ for $R_c = 6 \times 10^6$. The single Reynolds number reflects the limited test data available for these aerofoils. For $z_{u1.25}/c \geq 0.017$ Figure 4 gives ΔC_L as a function of $\tan \tau_u$ and R_c.

Figures 3 and 4 were obtained from measured data given in Derivations 2, 5 and 6, which covered the ranges of parameters given in Table 4.1. The aerofoils tested had leading-edge roughness as shown in Sketch 2.2a. Data presented in Derivation 9 reveal a loss in C_{Lm} due to simulated ice formation similar to that obtained due to leading-edge roughness. It is therefore considered that the data of Figures 3 and 4 can be used to indicate the loss of C_{Lm} due to ice formation by comparison with the corresponding values for smooth aerofoils obtained from Figures 1 and 2.

TABLE 4.1
Ranges of Parameters for Tests on Aerofoils with Rough Leading Edges

Parameter	*Range*
t/c	0.06 to 0.24
$z_{u1.25}/c$	0.0069 to 0.0563
$\tan \tau_u$	0.0429 to 0.2249
$R_c \times 10^{-6}$	0.7 to 6.0
M	0.09 to 0.15

5. LIFT COEFFICIENT AT ZERO INCIDENCE

The coefficient C_{L0} for use in Equation (2.1) is obtained by combining the lift-curve slope, $(a_1)_0$, for incompressible flow obtained from Item No. Aero W 01.01.05 (Reference 21) with the zero-lift angle, α_0, obtained by use of Pankhurst's method in Derivation 1,

$$\alpha_0 = -\frac{\pi}{90}\sum_{i=1}^{14}(B_i z_{ci}/c), \tag{5.1}$$

where

$$z_{ci} = [z_u(x_i/c) + z_l(x_i/c)]/2. \tag{5.2}$$

The coefficients B_i are specified in Table 5.1 for the required values of x_i/c.

TABLE 5.1

Coefficients B_i in Equation (5.1)

i	x_i/c	B_i	i	x_i/c	B_i
1*	0	1.45	8	0.50	3.67
2	0.025	2.11	9	0.60	4.69
3	0.05	1.56	10	0.70	6.72
4	0.10	2.41	11	0.80	11.75
5	0.20	2.94	12	0.90	21.72
6	0.30	2.88	13	0.95	99.85
7	0.40	3.13	14*	1.0	–164.88

* Note that for the present definition of chord line the terms $i = 1$ and 14 do not contribute to α_0.

Hence, the lift coefficient at zero incidence $(\alpha = 0)$ is given by

$$C_{L0} = -\alpha_0(a_1)_0. \tag{5.3}$$

Comparison with measured data in Derivations 2, 5, 8, 10 to 13, and 15 to 20 has shown this to be an adequate first approximation to C_{L0} and it is the method that must be used in the evaluation of C_{Lm} by Equation (2.1) in order to maintain the integrity of the original correlation. However, the issue of more recent Items, based on use of the VGK CFD code in the Transonic Aerodynamics Sub-series, means that the methods of Item Nos 72024, 97020 and 98011 (References 24 to 26), taken together, allow a more accurate evaluation of C_{L0} for use elsewhere. However, it may be noted that the difference in prediction is small in magnitude and of little consequence in the estimation of C_{Lm}.

6. FACTOR ON MAXIMUM LIFT COEFFICIENT FOR MODERN AEROFOILS

Analysis of measured data has revealed that modern, rear-loaded, aerofoils, which terminate with a small trailing-edge base and incorporate large rear camber, have a higher C_{Lm} than conventional aerofoils with the same $z_{u1.25}/c$ and $\tan\tau_u$.

The factor, F_S, for use in Equation (2.1), is obtained from Figure 5 as a function of R_c and is applied only for modern aerofoils. For conventional aerofoils $F_S = 1.0$. Figure 5, which was obtained by an analysis of data from Derivations 8, 11 to 13, 15, and 17 to 20, should be used with caution for aerofoils that differ significantly from those used in its derivation, which cover the ranges of geometry given in Table 6.1.

TABLE 6.1
Geometrical Ranges for Data Used to Derive Figure 5

Parameter	*Range*
t/c	0.13 to 0.21
$z_{u1.25}/c$	0.024 to 0.0383
$\tan\tau_u$	0.117 to 0.207
t_b/c	0.005 to 0.009
$[z_u(0.9) - z_l(0.9)]/z_u(0.9)$	0.64 to 1.14

Here, t_b is the trailing-edge base thickness (see Sketch 1.1) and $[z_u(0.9) - z_l(0.9)]/z_u(0.9)$ is a measure of the amount of rear camber.

7. MACH NUMBER FACTOR ON MAXIMUM LIFT COEFFICIENT

As Mach number increases there is a noticeable reduction in C_{Lm}. This reduction is more marked for aerofoils with smaller leading-edge radii, which have increased leading-edge peak suctions.

The Mach number factor, F_M, is given by

$$F_M = 1 - F_1 F_2, \tag{7.1}$$

where F_1 is given in Figure 6 as a function of M, and F_2 is given in Figure 7 as a function of the parameter $[z_u(0.05) - z_u(0.01)]/c$.

The parameters F_1 and F_2 are based on data from Derivations 7, 8, 10 to 12, 15, 16, and 18 to 20.

8. ACCURACY

The accuracy of the method presented in this Item can be assessed from a comparison of measured and estimated values of C_{Lm}. The data for comparison have been considered in groups corresponding to aerofoil type and surface condition and the standard deviations for each group are presented in Tables 8.1 to 8.5 below, which include the number of data points for each Reynolds number.

TABLE 8.1
NACA Conventional Symmetric Aerofoils – Smooth Leading Edge

R_c	*Standard Deviation*	*Number of Data Points*
1×10^6	0.065	2
2×10^6	0.055	2
3×10^6	0.068	27
6×10^6	0.047	27
9×10^6	0.061	27
All R_c	0.059	85

TABLE 8.2
NACA Conventional Cambered Aerofoils – Smooth Leading Edge

R_c	*Standard Deviation*	*Number of Data Points*
1×10^6	0.095	11
2×10^6	0.098	14
3×10^6	0.085	64
6×10^6	0.086	68
9×10^6	0.076	63
All R_c	0.084	220

TABLE 8.3
NASA Modern Cambered Aerofoils – Smooth Leading Edge
(including cases with minimum roughness, Sketch 2.1)

R_c	*Standard Deviation*	*Number of Data Points*
2×10^6	0.081	18
3×10^6	0.085	18
6×10^6	0.091	18
9×10^6	0.080	16
All R_c	0.084	70

TABLE 8.4
NACA Conventional Symmetric Aerofoils – Rough Leading Edge
(Sketch 2.2a)

R_c	*Standard Deviation*	*Number of Data Points*
1×10^6	0.045	2
2×10^6	0.081	2
6×10^6	0.082	27
All R_c	0.080	31

TABLE 8.5
NACA Conventional Cambered Aerofoils – Rough Leading Edge
(Sketch 2.2a)

R_c	*Standard Deviation*	*Number of Data Points*
1×10^6	0.051	10
2×10^6	0.051	10
6×10^6	0.096	67
All R_c	0.088	87

9. DERIVATION AND REFERENCES

9.1 Derivation

The Derivation lists selected sources that have assisted in the preparation of this Item.

1.	PANKHURST, R.C.	A method for the rapid evaluation of Glauert's expressions for the angle of zero lift and the moment at zero lift. ARC R & M 1914, 1944.
2.	ABBOTT, I.H. VON DOENHOFF, A.E. STIVERS, S.	Summary of airfoil data. NACA Rep. 824, 1945.
3.	LOFTIN, L.K. BURNSNALL, W.J.	The effect of variations in Reynolds number between 3.0×10^6 and 25.0×10^6 upon the aerodynamic characteristics of a number of NACA 6-series airfoil sections. NACA tech. Note 1773, 1948.
4.	GAULT, E.	A correlation of low-speed, airfoil-section stalling characteristics with Reynolds number and airfoil geometry. NACA tech. Note 3963, 1957.
5.	ABBOTT, I.H. VON DOENHOFF, A.E.	*Theory of wing sections, including a summary of airfoil data*. Dover Publications, New York, 1959.
6.	RIEGELS, F.W.	*Aerofoil sections.* Butterworth, London, 1961.
7.	VAN DEN BERG, B.	Reynolds number and Mach number effects on the maximum lift and the stalling characteristics of wings at low speeds. NLR tech. Rep. 69025U, 1969.
8.	McGHEE, R.J. BEASLEY, W.D.	Low-speed aerodynamic characteristics of a 17-percent-thick airfoil section designed for general aviation applications. NASA tech. Note D-7428, 1973.
9.	HOERNER, S.F. BORST, H.V.	*Fluid-dynamic lift.* Published by L.A. Hoerner, 1975.
10.	BEASLEY, W.D. McGHEE, R.J.	Experimental and theoretical low-speed aerodynamic characteristics of the NACA 65-213, $a = 0.50$, airfoil. NASA tech. Memor. X-3160, 1975.
11.	McGHEE, R.J. BEASLEY, W.D.	Effect of thickness on the aerodynamic characteristics of an initial low-speed family of airfoils for general aviation applications. NASA tech. Memor. X-72843, 1976.
12.	McGHEE, R.J. BEASLEY, W.D. SOMERS, D.M.	Low-speed aerodynamic characteristics of a 13-percent-thick airfoil section designed for general aviation applications. NASA tech. Memor. X-72697, 1977.
13.	McGHEE, R.J. BEASLEY, W.D.	Wind-tunnel results for an improved 21-percent-thick low-speed airfoil section. NASA tech. Memor. 78650, 1978.

14.	WILLMER, A.C.	Aerodynamic investigation into the feasibility of a 25 m vertical axis windmill. BAe Filton Aero. Rep. 124, 1979.
15.	McGHEE, R.J. BEASLEY, W.D.	Low-speed aerodynamic characteristics of a 13-percent-thick medium-speed airfoil designed for general aviation applications. NASA tech. Paper 1498, 1979.
16.	McGHEE, R.J. BEASLEY, W.D. WHITCOMB, R.T.	NASA low- and medium-speed airfoil development. NASA tech. Memor. 78709, 1979.
17.	McGHEE, R.J. BEASLEY, W.D.	Low-speed wind-tunnel results for a modified 13-percent-thick airfoil. NASA tech. Memor. X-74018, 1979.
18.	HARRIS, C.D. BEASLEY, W.D.	Low-speed aerodynamic characteristics of a 14-percent-thick NASA Phase 2 supercritical airfoil designed for a lift coefficient of 0.7. NASA tech. Memor. 81912, 1980.
19.	McGHEE, R.J. BEASLEY, W.D.	Low-speed aerodynamic characteristics of a 17-percent-thick medium-speed airfoil designed for general aviation applications. NASA tech. Paper 1786, 1980.
20.	McGHEE, R.J. BEASLEY, W.D.	Wind-tunnel results for a modified 17-percent-thick low-speed airfoil section. NASA tech. paper 1919, 1981.

9.2 References

The References list selected sources of information supplementary to that given in this Item.

21.	ESDU	Slope of lift curve for two-dimensional flow. ESDU International, Item No. Aero W.01.01.05, 1955.
22.	ESDU	The low-speed stalling characteristics of aerodynamically smooth aerofoils. ESDU International, Item No. 66034, 1966.
23.	ESDU	Program for calculation of maximum lift coefficient of plain aerofoils and wings at subsonic speeds. ESDU International, Item No. 93015, 1993.
24.	ESDU	Aerodynamic characteristics of aerofoils in compressible inviscid airflow at subcritical Mach numbers. ESDU International, Item No. 72024, 1972.
25.	ESDU	Slope of aerofoil lift curve for subsonic two-dimensional flow. ESDU International, Item No. 97020, 1997.
26.	ESDU	Aerofoil incidence for zero lift in subsonic two-dimensional flow. ESDU International, Item No. 98011, 1998.

10. EXAMPLES

10.1 Example 1

The maximum lift coefficient is to be estimated for a two-dimensional NACA 65-210 aerofoil section with a smooth leading edge. Estimates are required for Reynolds numbers of 3, 6 and 9 $\times$ 10^6 at a Mach number of 0.10. For the aerofoil it can be assumed that the trailing-edge angle, τ, is zero and that boundary layer transition occurs at 0.3*c*.

The required aerofoil surface ordinates have the following values.

TABLE 10.1

x/c	z_u/c	z_l/c	x/c	z_u/c	z_l/c
0	0	0	0.50	0.0592	–0.0371
0.01	0.012	–0.010	0.60	0.0522	–0.0308
0.0125	0.013	–0.0105	0.70	0.0413	–0.0218
0.025	0.018	–0.014	0.80	0.0278	–0.0119
0.05	0.025	–0.019	0.90	0.0133	–0.0029
0.10	0.036	–0.025	0.95	0.0062	0.0001
0.20	0.0495	–0.0334	0.99	0.00124	0.00002
0.30	0.0570	–0.0379	1.0	0	0
0.40	0.0607	–0.0392			

The procedure is first to calculate, from Section 5, the lift coefficient at zero incidence, C_{L0}, then to calculate the lift coefficient increment, ΔC_L, from Section 3. The values of C_{Lm} are then obtained from Equation (2.1) with factors $F_S = 1.0$ for a conventional aerofoil section and $F_M = 1.0$ for $M = 0.1$.

The calculations are carried out using the following steps.

(i) From Equation (5.1), Table 5.1 and Table 10.1 the zero-lift angle is calculated as

$$\alpha_0 = -0.0274 \text{ rad.}$$

(ii) From use of Reference 21 the values of $(a_1)_0$ are calculated.

(iii) The lift coefficient at zero incidence, C_{L0}, is calculated from Equation (5.3).

(iv) From Table 10.1 $z_{u1.25}/c = 0.013$ and ΔC_L is obtained from Figure 1.

(v) Finally, the values of C_{Lm} are evaluated using Equation (2.1) which, with $F_S = 1$ and $F_M = 1.0$, simplifies to

$$C_{Lm} = C_{L0} + \Delta C_L .$$

The results of the calculations are summarised in Table 10.2.

TABLE 10.2

R_c	3×10^6	6×10^6	9×10^6
$(a_1)_0$	5.89	6.01	6.06
C_{L0}	0.161	0.164	0.166
ΔC_L	1.122	1.194	1.234
C_{Lm}	1.28	1.36	1.40

10.2 Example 2

The effect of coarse surface roughness or ice formation over the leading edge on the maximum lift coefficient is to be estimated for the aerofoil of Example 1.

The Reynolds number is 6×10^6 and the Mach number is 0.1.

It can be assumed that the roughness shifts the boundary layer transition forward to the leading edge.

From Example 1, $C_{Lm} = 1.36$ for the aerofoil with a smooth leading edge.

For the aerofoil with a rough leading edge the procedure of Example 1 is followed but with the lift increment, ΔC_L, being obtained from Figure 3.

In this case with $z_{u1.25}/c = 0.013$ the value of ΔC_L is 0.886. Also, the effect of the shift in boundary layer transition gives a slightly reduced C_{L0} value of 0.163.

Thus,
$$\begin{aligned} C_{Lm} &= C_{L0} + \Delta C_L \\ &= 0.163 + 0.886 \\ &= 1.05\,. \end{aligned}$$

The loss in C_{Lm} due to coarse leading-edge roughness or ice formation is given by

$$\Delta C_{Lm} = 1.36 - 1.05 = 0.31\,.$$

This page Amendment C

10.3 Example 3

The effect of Mach number on the maximum lift coefficient is to be estimated for the aerofoil used in Example 1 with a smooth leading edge. Estimates are required for Mach numbers up to 0.4 at a Reynolds number of 6×10^6.

The values of C_{Lm} are estimated using Equation (2.1) which, with $F_S = 1.0$, simplifies to

$$C_{Lm} = (C_{L0} + \Delta C_L)F_M .$$

From Example 1, $(C_{L0} + \Delta C_L) = 1.36$.

The factor F_M is obtained from Equation (7.1), *i.e.*

$$F_M = 1 - F_1 F_2 ,$$

in which F_1 is found from Figure 6 and F_2, from Figure 7, corresponds to

$$[z_u(0.05) - z_u(0.01)]/c = 0.013 .$$

The calculations are tabulated in Table 10.3.

TABLE 10.3

M	0.1	0.2	0.3	0.4
F_1 (Figure 6)	0	0.036	0.100	0.141
F_2 (Figure 7)	2.07	2.07	2.07	2.07
F_M (Equation (7.1))	1.0	0.925	0.793	0.708
C_{Lm}	1.36	1.26	1.08	0.96

LIFT COEFFICIENT INCREMENT FOR AEROFOILS WITH SMOOTH LEADING EDGES

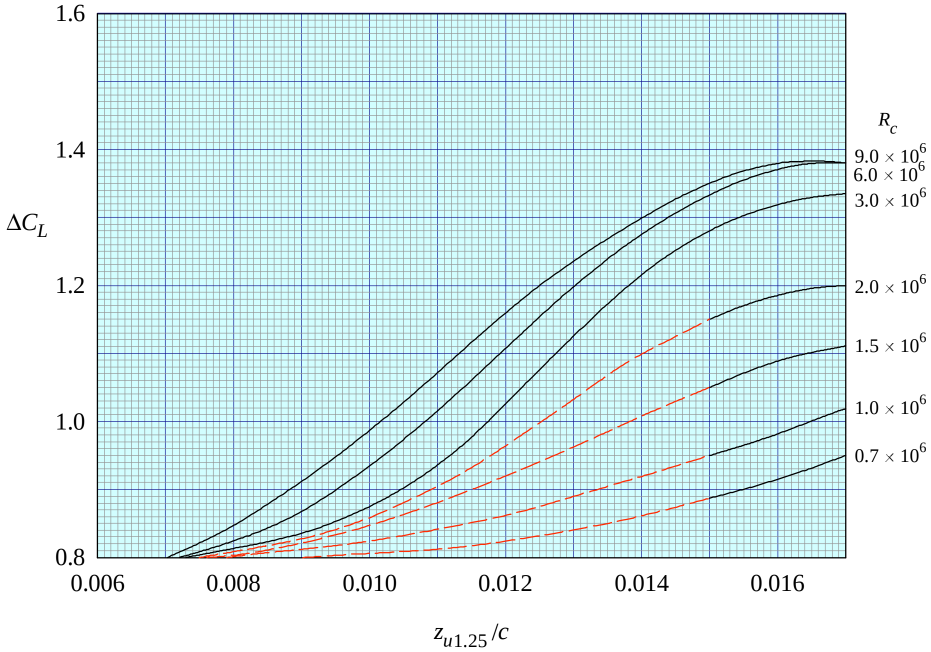

FIGURE 1 $z_{u1.25}/c < 0.017$

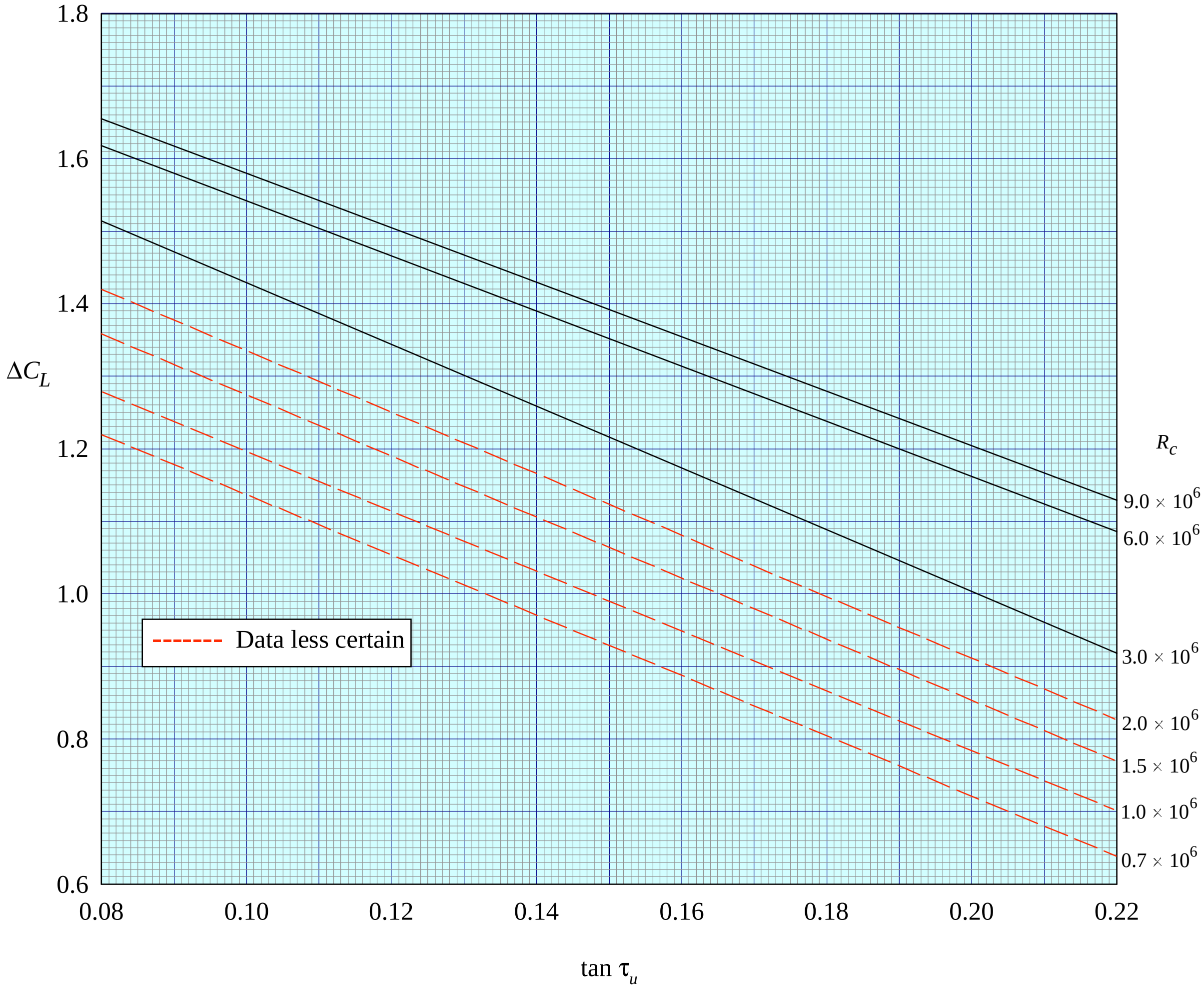

FIGURE 2 $z_{u1.25}/c \geq 0.017$

This page Amendment C

LIFT COEFFICIENT INCREMENT FOR AEROFOILS WITH ROUGH LEADING EDGES

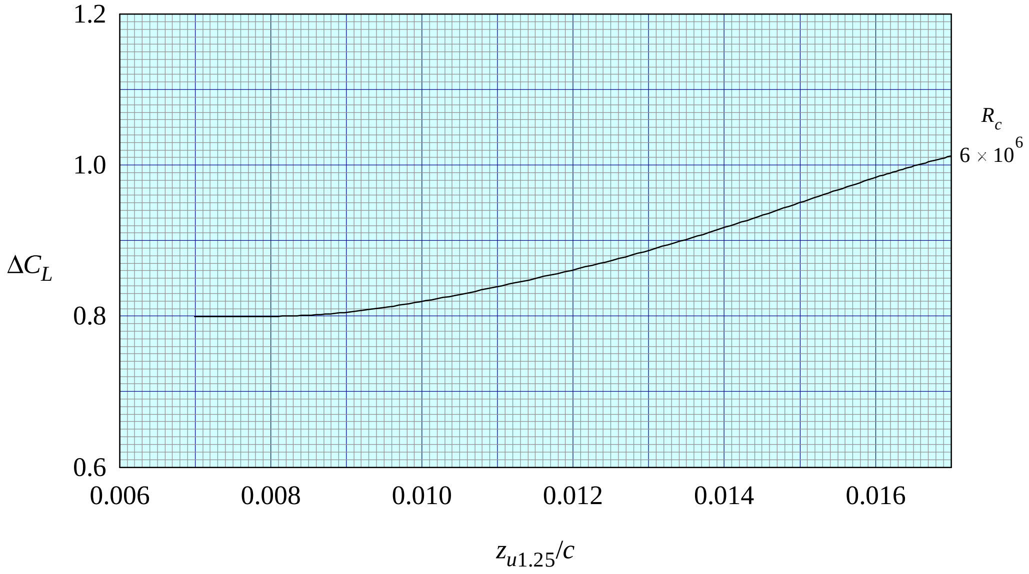

FIGURE 3 $z_{u1.25}/c < 0.017$

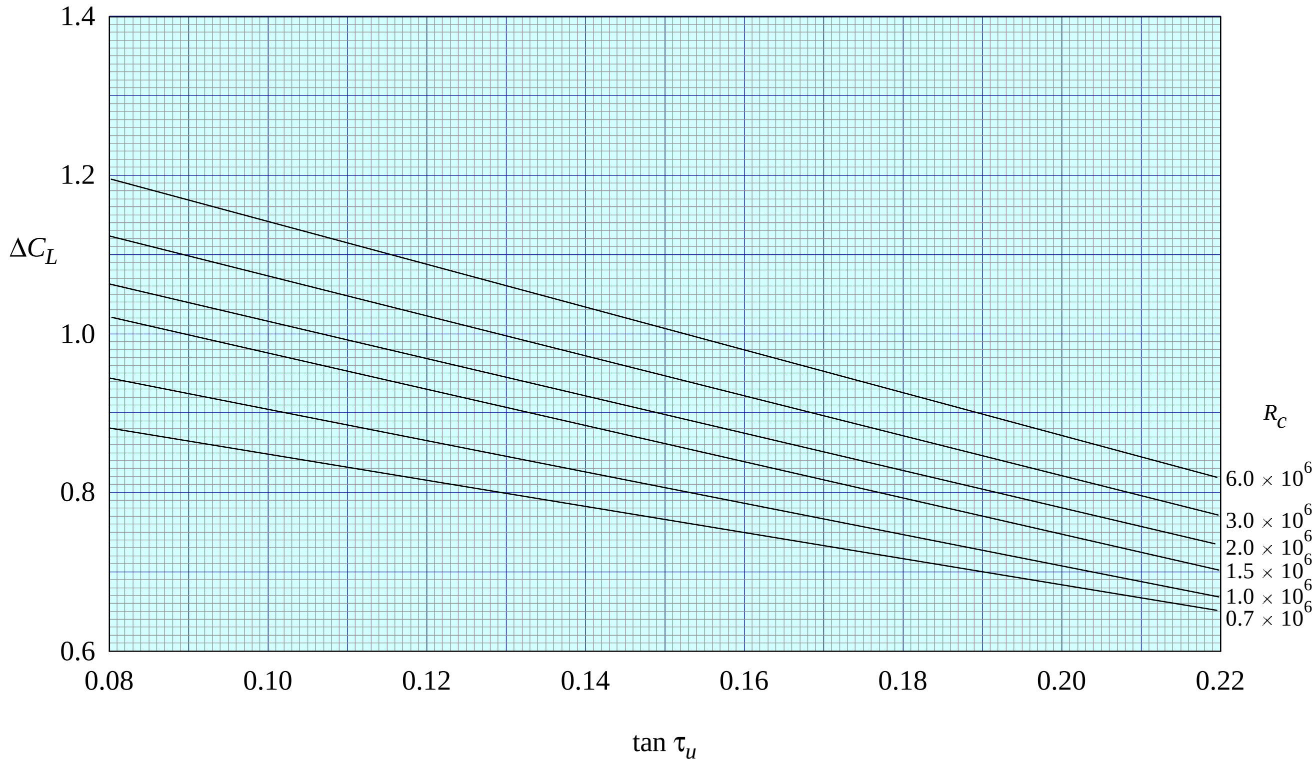

FIGURE 4 $z_{u1.25}/c \geq 0.017$

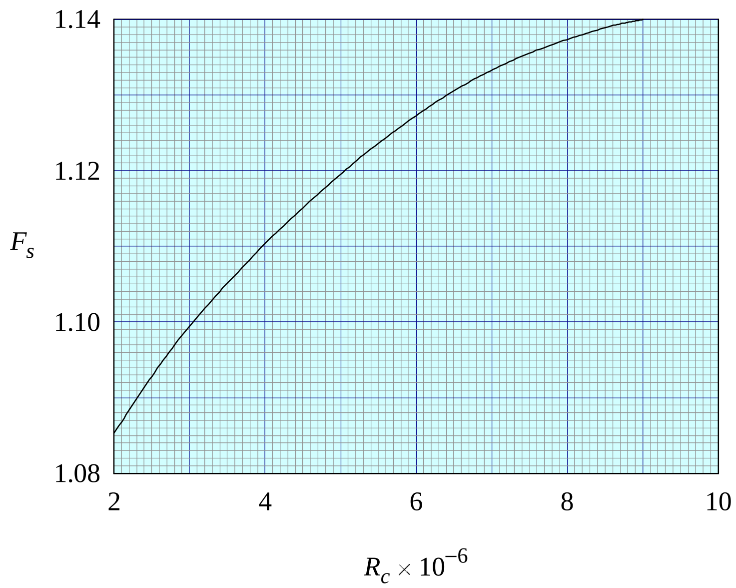

FIGURE 5 FACTOR ON C_{Lm} FOR MODERN AEROFOILS

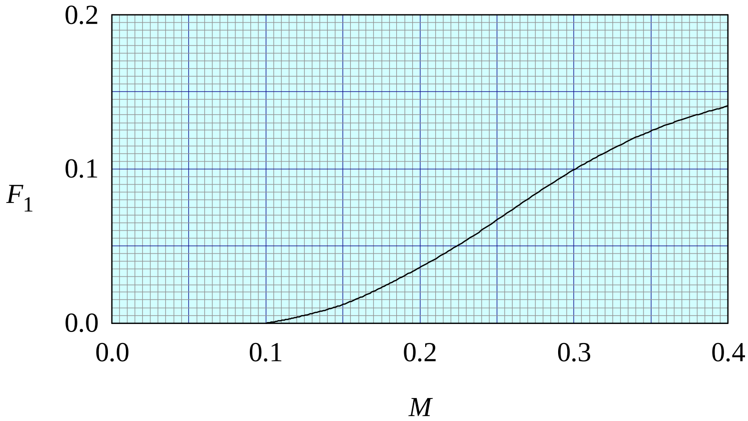

FIGURE 6 PARAMETER IN EQUATION (7.1)

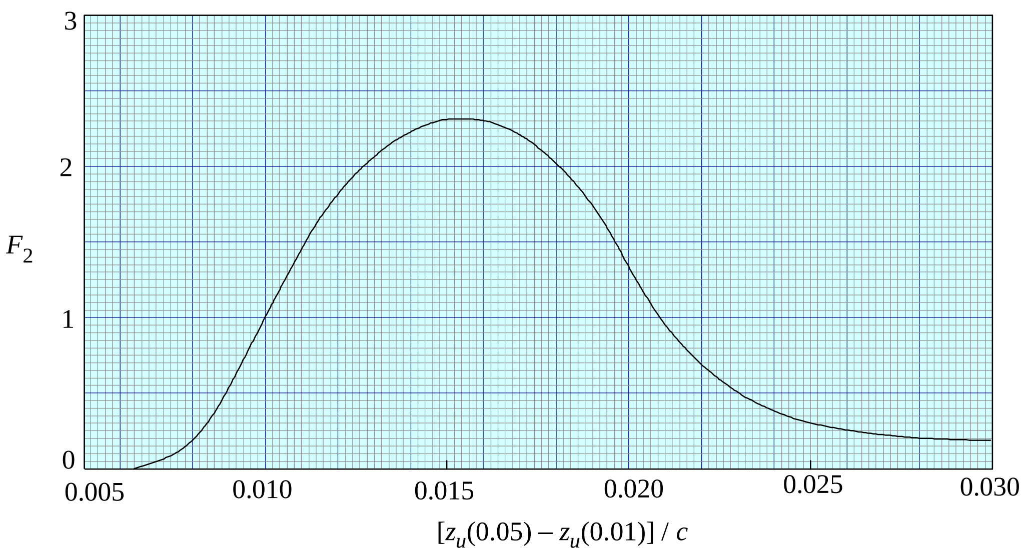

FIGURE 7 PARAMETER IN EQUATION (7.1)

THE PREPARATION OF THIS DATA ITEM

The work on this particular Item, which supersedes Item No. Aero W.01.01.06, was monitored and guided by the Aerodynamics Committee, which first met in 1942 and now has the following membership:

Chairman		
Mr H.C. Garner	–	Independent
Vice-Chairman	–	
Mr P.K. Jones	–	British Aerospace plc, Aircraft Group, Manchester
Members		
Mr D. Bonenfant	–	Aérospatiale, Toulouse, France
Mr E.A. Boyd	–	Cranfield Institute of Technology
Mr K. Burgin	–	Southampton University
Mr E.C. Carter	–	Aircraft Research Association
Mr J.R.J. Dovey	–	British Aerospace plc, Aircraft Group, Warton
Dr J.W. Flower	–	Bristol University
Mr A. Hipp	–	British Aerospace plc, Dynamics Group, Stevenage
Mr J. Kloos*	–	Saab-Scania, Linköping, Sweden
Mr J.R.C. Pedersen	–	Independent
Mr I.H. Rettie*	–	Boeing Aerospace Company, Seattle, Wash., USA
Mr A.E. Sewell*	–	Northrop Corporation, Hawthorne, Calif., USA
Mr F.W. Stanhope	–	Rolls-Royce Ltd, Derby
Mr H. Vogel	–	British Aerospace plc, Aircraft Group, Weybridge.

* Corresponding Members

The technical work involved in the initial assessement of the available information and the construction and subsequent development of the Item was carried out under contract to ESDU by Mr C.D. Hollis and Mr R.G. Williams of British Aerospace plc, Aircraft Group, Bristol.